Available online at www.sciencedirect.com
ScienceDirect
Ceramics International 37 (2011) 3731–3735
CERAMICS INTERNATIONAL
www.elsevier.com/locate/ceramint

Short communication

Mechanical synthesis and characterization of $Bi_4Ti_3O_{12}$ nanopowders

R. Anlin Golda [a], A. Marikani [b,*], D. Pathinettam Padiyan [c]

[a] Department of Nanoscience and Technology, Mepco Schlenk Engineering College, Sivakasi 626 005, Virudhunagar District, Tamil Nadu, India
[b] Department of Physics, Mepco Schlenk Engineering College, Sivakasi 626 005, Virudhunagar District, Tamil Nadu, India
[c] Department of Physics, Manonmaniam Sundaranar University, Tirunelveli 627 012, Tamil Nadu, India

Received 1 April 2011; received in revised form 27 April 2011; accepted 28 April 2011
Available online 6 May 2011

Abstract

Nanocrystalline bismuth titanate (BiT) powders with the particle size distribution in the range of 30–45 nm were synthesized from their oxides Bi_2O_3 and TiO_2 using mechanical ball milling process. The ball milling synthesis was performed in air for 5 h. The synthesized BiT ceramic was calcined at 900 °C in air atmosphere for 2 h without a pre-calcination step. The X-ray diffraction pattern was used to analyze the formations of phase and crystal structure. The morphology and the microstructure of the nanosized bismuth titanate powders were studied using scanning electron microscope. The Raman spectrum measurement was used to investigate the structural changes observed in the formation of BiT nanopowders. The photoluminescence measurement showed that the material exhibited maximum emissions at 454 nm and 469 nm in the visible emission band around blue–green colour.

Keywords: $Bi_4Ti_3O_{12}$; Nanopowders; Ball milling; ac impedance; Photoluminescence; Raman study

1. Introduction

Bismuth titanate ($Bi_4Ti_3O_{12}$) belongs to Aurivillius family with a general formula of $(Bi_2O_2)[A_{m-1}(B)_mO_{3m+1}]$, which consists of $(Bi_2Ti_3O_{10})^{2-}$ layers sandwiched between bismuth oxide $(Bi_2O_2)^{2+}$ layers [1]. BiT has relatively high dielectric permittivity (~200), very high Curie temperature [T_C = 675 °C], and breakdown strength [2]. It is an interesting lead-free ferroelectric material with layered structure and environmental friendly ceramic with potential applications in electronic industry as capacitors, sensors, memory storage devices, optical display and other electro-optical devices [3,4]. Studies on BiT shows that it has a high leakage current and domain pinning due to defects such as Bi vacancies accompanied by oxygen vacancies [5,6]. Furthermore, it suffers from a low durability against a repeated switching of polarization states [7], which is probably ascribed to lattice defects [8,9]. These electrical properties prevent it from practical ferroelectric random access memory (FRAM) and piezoelectric applications.

Recently, efforts have been devoted to study $Bi_4Ti_3O_{12}$ ceramics and thin films fabricated by various methods. The bismuth titanate powder is prepared using the conventional ceramic route such as solid state reaction method [10]. This conventional method produces non-stoichiometric composition due to the undesirable loss of bismuth content through volatilization at elevated temperature. In addition, it also produces crystallites coarsening and particle aggregation due to calcination at high temperature.

Hence, many chemical methods such as hydrothermal method [11], sol–gel processes [12,13], coprecipitation method [14], the microemulsion method [15], the metal–organic polymeric precursor process [16] and so on have been investigated as alternatives. The advantages of the chemical methods over the other methods are the controlled morphology, narrow particle size distribution, high purity, high crystallinity, and possible reduction in sintering temperatures. However, the chemistry based methods use moisture or light sensitive chemicals, such as bismuth salts, that make them difficult to deal with.

Among the various techniques available for the synthesis of BiT powders, the mechanical alloying has certain advantages such as low cost and it uses widely available oxides as the starting materials and skips the calcination steps at intermediate

* Corresponding author. Tel.: +91 4562 235690; fax: +91 4562 235111.
E-mail addresses: amari@mepcoeng.ac.in, amarikani_phy@yahoo.co.in (A. Marikani).

0272-8842/$36.00
doi:10.1016/j.ceramint.2011.04.123

temperatures, leading to a simplified process [17]. Recently, the literature has reported few studies on the mechanical synthesis of the layered structures such as $Bi_4Ti_3O_{12}$ [18,19]. Therefore, in this study, BiT powders were prepared by mechanical ball milling method and heat treated at 900 °C for 2 h. The lattice parameters, ac impedance, Raman spectrum, and photoluminescence of BiT nanopowders were studied using different characterization techniques.

2. Experimental procedure

The bismuth titanate was prepared using commercially available chemicals bismuth oxide (Bi_2O_3) and titanium dioxide (TiO_2) as the starting materials. The stoichiometric composition of the bismuth titanate was prepared by taking 3% excess of Bi_2O_3. The required Bi_2O_3 and TiO_2 chemicals were weighed and loaded in a tungsten jar together with tungsten milling balls of 10 mm in diameter. The mechanically assisted synthesis was performed in a planetary ball mill (Pulverisette 6, Fritsch make, Germany) with the following milling conditions: ball to powder weight ratio 20:1, the basic disc rotation speed was 317 min^{-1}, the rotation of the disc with jar was 396 min^{-1} and milling time 5 h. The obtained bismuth titanate powder was sintered in a furnace at 900 °C for 2 h with the heating rate of 10 °C min^{-1}.

The powder X-ray diffraction (XRD) was performed for the sintered powder using a XPERT-PRO X-ray diffractometer (42 kV, 30 mA) with Cu Kα radiation (λ = 0.15406 nm). The ac impedance analysis was measured using SR830DSP Lock-in-amplifier, in the frequency range 1 Hz to 100 kHz. For ac impedance measurement, 1 g of sintered bismuth titanate powder was used to produce a pellet with a size 12 mm diameter using a hydraulic press with an applied pressure of 3 tonnes. The pelletized sample is placed between two copper electrodes. The FTIR spectra were recorded at room temperature (300 K) from 400 to 4000 cm^{-1} using FTIR spectrophotometer (Bruker make, Alpha-E model, Germany). The surface micrograph of the sintered powder was studied using a scanning electron microscope (PHILIPS make, model-XL30). The surface roughness and morphology was characterized by AFM (Scanning Probe microscope, PHILIPS make, and model-XL30) in non-contact mode. The Raman spectrum was measured using from 0 cm^{-1} to 1500 cm^{-1} using Raman Spectrometer (Jobin Yuon model HR-300) equipped with He–Ne laser of wavelength 632.8 nm. The photoluminescence was measured from 380 nm to 600 nm using Spectrofluorophotometer (Model No.: R7-5301 PC, Shimadzu, Japan).

3. Results and discussion

3.1. Structure and morphology

The X-ray diffraction pattern recorded for the milled $Bi_4Ti_3O_{12}$ nanopowder sintered at 900 °C is shown in Fig. 1. The XRD peaks were indexed using the JCPDS files [JCPDS card No.: 35-0795] [20]. The bismuth titanate nanopowders crystallizes into orthorhombic lattice with lattice constants, $a = 5.427$ Å, $b = 32.736$ Å and $c = 5.396$ Å. The lattice constants of bismuth titanate reported in the literature are $a = 5.448$ Å, $b = 32.81$ Å and $c = 5.41$ Å [20]. The good agreement of the obtained lattice constants with the standard values indicates that a single phase of $Bi_4Ti_3O_{12}$ with orthorhombic structure was obtained due to calcinations at 900 °C. The peaks centered at 2θ of 23.53°, 30.26°, 33.09°, and 33.33°, which are strongest, can correspond to orthorhombic structure (*h k l*) planes of (1 1 1), (1 1 7), (2 0 0) and (0 0 2) of $Bi_4Ti_3O_{12}$.

The SEM images recorded for the bismuth titanate nanopowders prepared by ball milling (5 h) before and after calcination are shown in Fig. 2a and b, respectively. Fig. 2a shows agglomeration of powder. Due to indistinct images, it is very difficult to determine the individual particle size. Therefore, the particle size was calculated using Scherrer's formula and it was found to be 45 nm. The morphology of the calcined BiT powder is plate-like grain structure. The AFM image recorded for the calcined bismuth titanate nanopowders

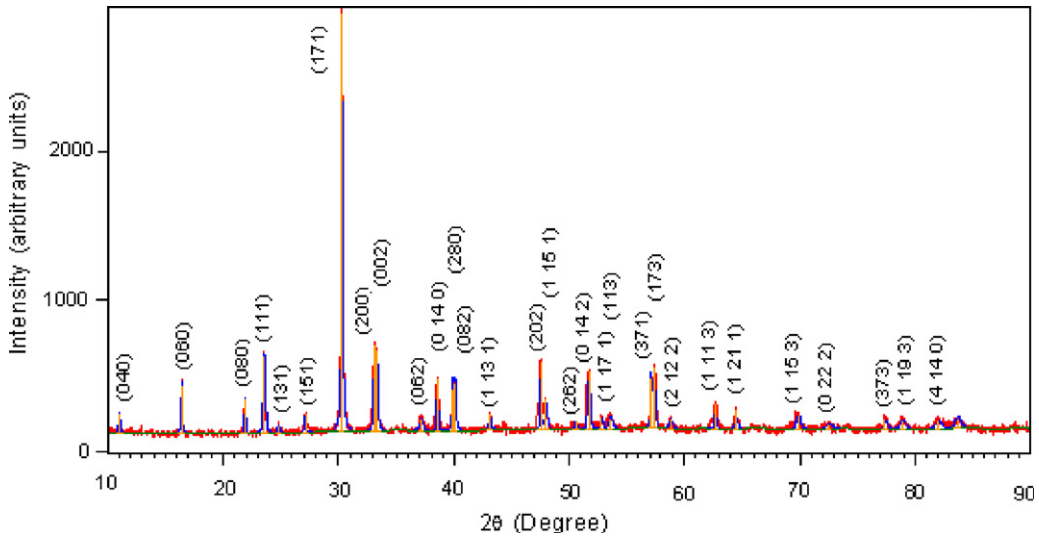

Fig. 1. X-ray diffraction pattern of nanocrystalline $Bi_4Ti_3O_{12}$ powder sintered at 900 °C.

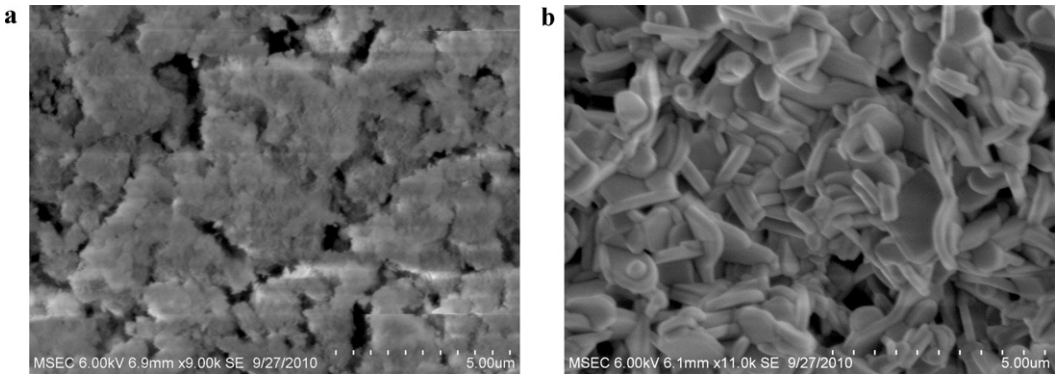

Fig. 2. SEM images of nanocrystalline $Bi_4Ti_3O_{12}$ powder, (a) as-synthesized, and (b) sintered at 900 °C for 2 h.

sintered at 900 °C is shown in Fig. 3. The AFM image shows that there is a grain growth in the calcined bismuth titanate nanopowder. The average grain size obtained from the AFM image of the calcined bismuth titanate nanopowders varies from 30 nm to 40 nm.

3.2. FTIR spectra

The FTIR spectra recorded at room temperature in the range 400–4000 cm^{-1} for the as-synthesized and the nanopowders sintered at 900 °C are compared in Fig. 4. The sharp peak at 1386 cm^{-1} for as-synthesized sample is assigned to the C=O and C≡O and it represents the presence of carbonates. The incorporation of carbonates in the as-synthesized $Bi_4Ti_3O_{12}$ nanopowders was due to the ethanol added as an additive during ball milling process. The peak at 645 cm^{-1} for as-synthesized sample is assigned to M–O vibrations. The absence of the band at 1386 cm^{-1} in the spectrum recorded for the calcined BiT powder indicates that the absence of carbonates in the calcined powder. The sharp absorption peaks for the calcined BiT powder at 817 cm^{-1}, the shoulder at 548 cm^{-1} and the peaks appearing in 479 cm^{-1} and 447 cm^{-1} are attributed to Ti–O stretching vibrations, which are in accordance with the results for $Bi_4Ti_3O_{12}$ reported in the literature [21,22]. The formation of a titanate structure is confirmed with characteristics bands below 830 cm^{-1}.

3.3. Impedance analysis

The impedance plot is drawn between the imaginary part of impedance (Z'') and the real part of impedance (Z') over a frequency range of 1–100 Hz at room temperature and it is shown in Fig. 5. The impedance data are explained through an equivalent circuit. This complex impedance plot is known as Nyquist plot and it typically consists of only one semicircle that indicates the presence of a single relaxation process. The single arc of the impedance spectrum representing a single RC element and hence from the impedance plot the relaxation frequency is determined. The maximum frequency that satisfies the condition $2\pi f_o R_b C_b = 1$ in the Nyquist plot is known as the relaxation frequency, where R_b is the bulk resistance, C_b is the bulk capacitance and f_o is the frequency at maximum of the semicircle. The bulk capacitance of the sample is calculated using the relation, $C_b = 1/(2\pi f_o R_b)$. The bulk electrical conductivity of the sample, $\sigma_o = t/(R_b A)$ where t is the thickness of the sample, and A is the area of the sample. The parameters evaluated from impedance measurements are as follows: bulk capacitance ~57.67 μF, bulk resistance ~6.9 MΩ, relaxation

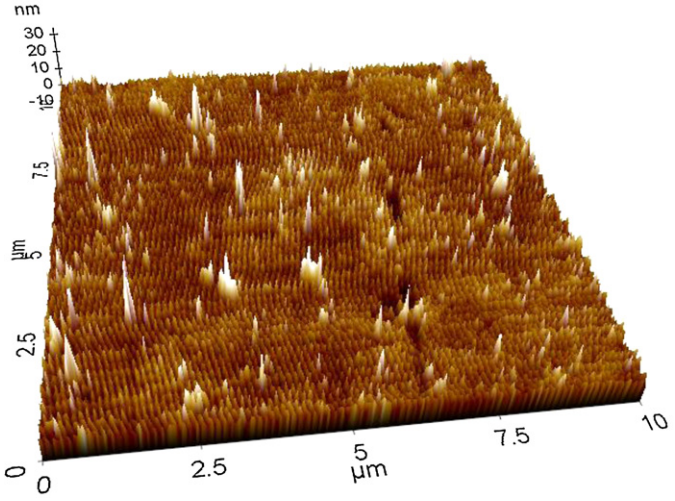

Fig. 3. AFM image of the nanocrystalline $Bi_4Ti_3O_{12}$ powder sintered at 900 °C.

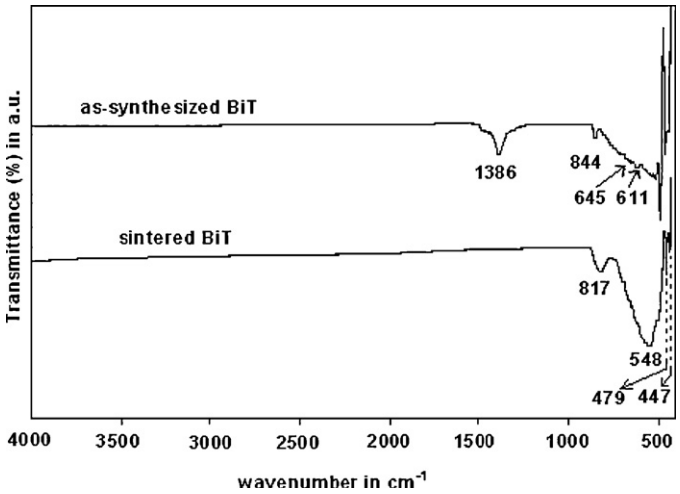

Fig. 4. FTIR spectra of nanocrystalline $Bi_4Ti_3O_{12}$ powders.

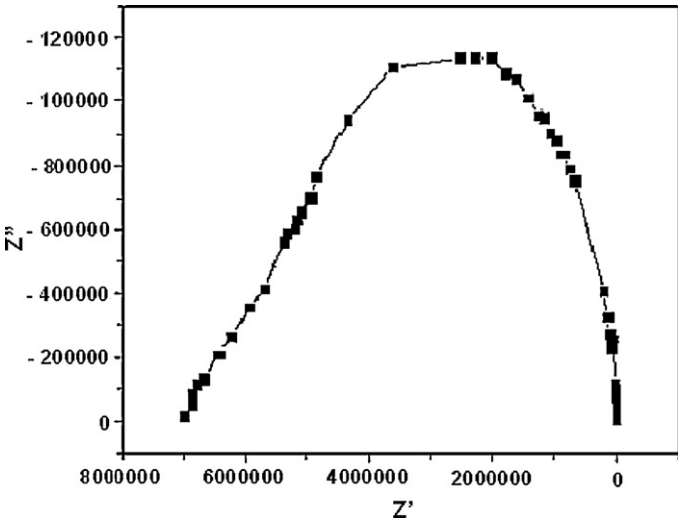

Fig. 5. Impedance plot of nanocrystalline $Bi_4Ti_3O_{12}$ powders.

frequency ~400 Hz, dielectric constant ~25, dielectric loss factor ~0.451 and ac conductivity ~$5.725 \times 10^{-7}\ \Omega^{-1}\ m^{-1}$.

3.4. Raman study

Raman spectroscopy is a useful tool to investigate the structural changes observed in the formation of BiT from ball milling. The Raman spectrum recorded for the bismuth titanate nanopowders annealed at 900 °C for 2 h is shown in Fig. 6. The Raman selection rule allows 24 Raman active modes for the orthorhombic BiT [23]. However, the Raman spectrum shown in Fig. 6 contains less number of Raman modes, which is partially due to the possibility of the same symmetry vibrations or weak features of some Raman bands [24].

The Raman data of our BiT powder sample is in good agreement with the earlier results, even though it is not quite exact for the mode counting in polycrystalline material due to possible symmetry breaking, low peak intensity, and overlap of vibration modes [25]. The Raman modes observed at 543 cm^{-1}, 616 cm^{-1} and 856 cm^{-1} are due to the high intra-group binding energy into the TiO_6 octahedral [26,27]. The Raman mode located at 275 cm^{-1} is ascribed to the Ti–O torsional-bending vibration modes into the TiO_6 octahedral, while the modes

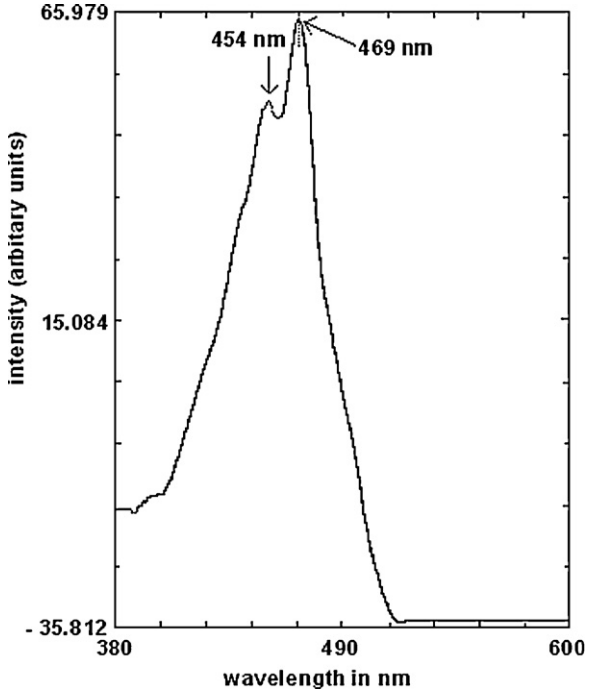

Fig. 7. Photoluminescence spectrum of nanocrystalline $Bi_4Ti_3O_{12}$ powders.

situated at 566 cm^{-1} and 856 cm^{-1} correspond to the O–Ti–O stretching modes [27]. The Raman mode at 233 cm^{-1} was ascribed to the O–Ti–O bending vibration. According to the symmetry of TiO_6, the mode at 233 cm^{-1} is Raman inactive, it is often observed because of the distortion of the octahedron. The mode at 336 cm^{-1} was from a combination of stretching and bending vibrations. Some phonon modes, e.g., at 336 cm^{-1}, 543 cm^{-1}, 616 cm^{-1} and 856 cm^{-1}, appear as wide and weak because of the considerable distortion in the TiO_6 octahedral and hence these phonon modes may induce stresses in crystalline BiT. The appearance of 275, 543 and 856 cm^{-1} suggests the presence of perovskite structure. Thus these powders exhibit an orthorhombic structure that is in agreement with XRD.

3.5. Photoluminescence

The photoluminescence spectrum recorded at room temperature for the milled $Bi_4Ti_3O_{12}$ nanopowders sintered at

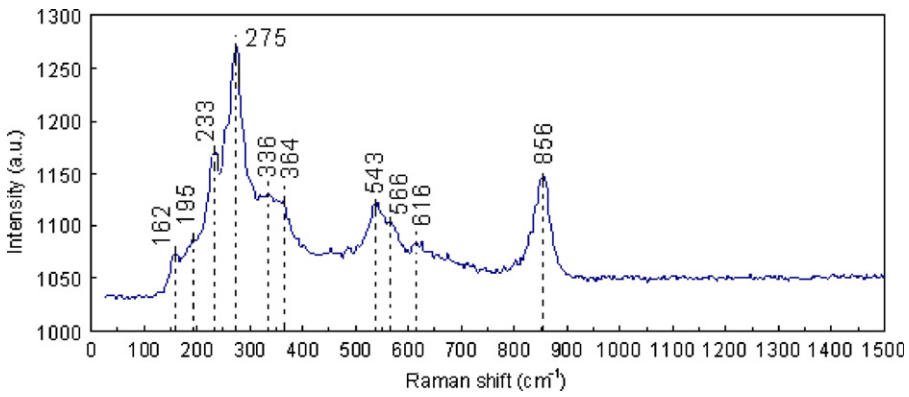

Fig. 6. Raman spectrum of nanocrystalline $Bi_4Ti_3O_{12}$ powders.

900 °C is shown in Fig. 7. The excitation energy of the photoluminescence spectrum is found to be 2.95 eV (420 nm). The maximum emission of photoluminescence occurs at 454 nm and 469 nm in a visible emission band around blue-green colour. In the case of nanocrystals, the origin of photoluminescence is due to the dominant role of the surface states, since there are a large number of unsaturated atoms existing in the surface regions of nanometer crystallites and forming localized levels within the forbidden gap of the materials. The quantum size effects and the oxygen vacancies could play a dominant role in the luminescence processes.

4. Conclusion

In summary, $Bi_4Ti_3O_{12}$ nanopowders with an average diameter in the range of 30–45 nm were synthesized using ball milling technique and then calcined at 900 °C for 2 h. The X-ray diffraction study shows that the calcined powder exhibits a single phase and it crystallizes into orthorhombic crystal structures. The SEM study shows that the bismuth titanate nanopowders calcined at 900 °C for 2 h exhibited plate-like morphology. The ac impedance measurement shows that the bismuth titanate nanopowders exhibited a single relaxation process. The Raman spectrum also confirms the orthorhombic crystal structure of the milled nanocrystalline bismuth titanate powders. The nanocrystalline bismuth titanate powders exhibited photoluminescence.

Acknowledgements

The authors (R.A. and A.M.) are grateful to Dr. S. Balakrishnan, Principal, and Thiru A. Tenzing, Correspondent, Mepco Schlenk Engineering College, Sivakasi for providing constant encouragement and support during this work.

References

[1] B. Aurivillius, Mixed bismuth oxides with layer lattices II – structure of $Bi_4Ti_3O_{12}$, Arkiv. Kemi. 1 (1949) 499–512.
[2] T. Takenaka, T. Gotoh, S. Mutoh, T. Sasaki, A new series of bismuth layer-structured ferroelectrics, Jpn. J. Appl. Phys. Part 1 34 (1995) 5384.
[3] T. Watanabe, H. Funakubo, M. Osada, Y. Noguchi, M. Miyayama, Effect of co-substitution of La and V in $Bi_4Ti_3O_{12}$ thin films on low-temperature deposition, Appl. Phys. Lett. 80 (1) (2002) 100–102.
[4] D. Wu, A.D. Li, T. Zhou, Z.G. Liu, N. Ming, Electrical properties of $Bi_{3.25}La_{0.75}Ti_3O_{12}$ thin films prepared by chemical–solution deposition, J. Appl. Phys. 88 (15) (2000) 5941–5945.
[5] W.C. Stewart, L.S. Cosentino, Some optical and electrical switching characteristics of a lead zirconate titanate ferroelectric ceramic, Ferroelectrics 1 (1970) 149–153.
[6] R. Lohkämper, H. Neumann, G. Arlt, Internal bias in acceptor-doped $BaTiO_3$ ceramics: numerical evaluation of increase and decrease, J. Appl. Phys. 68 (1990) 4220–4224.
[7] P.C. Joshi, S.B. Krupanidhi, Switching, fatigue and retention in ferroelectric $Bi_4Ti_3O_{12}$ thin films, Appl. Phys. Lett. 62 (1993) 1928–1930.
[8] Y. Noguchi, I. Miwa, Y. Goshima, M. Miyayama, Defect control for large remanent polarization in bismuth titanate ferroelectrics-doping effect of higher-valent cations, Jpn. J. Appl. Phys. 39 (2000) L1259–1262.
[9] W.L. Warren, B.A. Tuttle, D. Dimos, Ferroelectric fatigue in perovskite oxides, Appl. Phys. Lett. 67 (1995) 1426–1428.
[10] B.D. Stojanovic, C.O. Paiva-Santos, C. Jovalekic, A.Z. Simoes, F.M. Filho, Z. Lazarevic, J.A. Varela, Mechanically activating formation of layered structured bismuth titanate, Mater. Chem. Phys. 96 (2006) 471–476.
[11] P. Pookmanee, P. Uriwilast, S. Phanichpant, Hydrothermal synthesis of fine bismuth titanate powders, Ceram. Int. 30 (2004) 1913–1915.
[12] W.-F. Su, J.-F. Lee, M.Y. Chen, R.-M. Ho, Bismuth titanate nanoparticles dispersed polyacrylates, J. Mater. Res. 19 (2004) 2343–2348.
[13] N.V. Giridharan, S. Madeswaran, R. Jayavel, Structural, morphology and electrical studies on ferroelectric bismuth titanate thin films prepared by sol–gel technique, J. Cryst. Growth 237–239 (2002) 468–472.
[14] P. Pookmanee, S. Phanichpant, Characterization of lead-free bismuth titanate ($Bi_4Ti_3O_{12}$) synthesized by a modified oxalate co-precipitation method, J. Ceram. Process. Res. 10 (2009) 448–452.
[15] L. Xie, J. Ma, Z. Zhao, H. Tian, J. Zhou, Y. Wang, J. Tao, X. Zhu, A novel method for the preparation of $Bi_4Ti_3O_{12}$ nanoparticles in w/o microemulsion, Colloid Surf. A 280 (2006) 232–236.
[16] J. Hou, R.V. Kumar, Y. Qu, D. Krsmanovic, Controlled synthesis of photoluminescent $Bi_4Ti_3O_{12}$ nanoparticles from metal–organic polymeric precursor, J. Nanopart. Res. 12 (2010) 563–571.
[17] L.B. Kong, J. Ma, W. Zhu, O.K. Tan, Preparation of $Bi_4Ti_3O_{12}$ ceramics via a high-energy ball milling process, Mater. Lett. 51 (2001) 108.
[18] J. Wang, J.M. Xue, D.M. Wan, B.K. Gan, Mechanically activating nucleation and growth of complex perovskites, J. Solid State Chem. 154 (2000) 321.
[19] B.D. Stojanoviĉ, C.O. Paiva-Santos, M. Cilense, C. Jovalekiĉ, Z.Ź. Lazarević, Structure study of $Bi_4Ti_3O_{12}$ produced via mechanochemically assisted synthesis, Mater. Res. Bull. 43 (2008) 1743–1753.
[20] JCPDS Card No.: 35-0795.
[21] D. Chen, X. Jiao, Hydrothermal synthesis and characterization of $Bi_4Ti_3O_{12}$ powders from different precursors, Mater. Res. Bull. 36 (2001) 355–363.
[22] Y. Kan, P. Wang, Y. Li, Y.B. Cheng, D. Yan, Low-temperature sintering of $Bi_4Ti_3O_{12}$ derived from co-precipitation method, Mater. Lett. 56 (2002) 910–914.
[23] Q. Yang, Y. Li, Q. Yin, P. Wang, Y.B. Cheng, $Bi_4Ti_3O_{12}$ nanoparticles prepared by hydrothermal synthesis, J. Eur. Ceram. Soc. 23 (2003) 161–166.
[24] H. Idink, V. Srikanth, W.B. White, E.C. Subbarao, Raman study of low temperature phase transitions in bismuth titanate, $Bi_4Ti_3O_{12}$, J. Appl. Phys. 76 (1994) 1819–1823.
[25] W.L. Liu, H.R. Xia, H. Han, X.Q. Wang, Structural and dielectrical properties of bismuth titanate nanoparticles prepared by metalorganic decomposition method, J. Cryst. Growth 269 (2004) 499–504.
[26] M. Osada, M. Tada, M. Kakihana, T. Watanabe, H. Funakubo, Cation distribution and structural instability in $Bi_{4-x}La_xTi_3O_{12}$, Jpn. J. Appl. Phys. 40 (2001) 5572–5575.
[27] N. Sugita, M. Osada, E. Tokumitsu, Characterization of sol–gel derived $Bi_{4-x}La_xTi_3O_{12}$ films, Jpn. J. Appl. Phys. 41 (2002) 6810–6813.